

ANALYSIS OF A LINEAR SCHEME FOR ESTIMATION OF LOCAL ANISOTROPY FROM P-WAVE DATA IN MULTI-AZIMUTH VSP SURVEYS

Raiza de Nazaré Assunção Macambira, Ellen de Nazaré Souza Gomes
and Adriano César Rodrigues Barreto

ABSTRACT. This study presents an analysis of the linear inversion scheme for estimating anisotropy in the neighborhood of a receiver placed in a well using the vertical components of the slowness and polarization vectors of P-waves measured in multi-azimuth walkaway vertical seismic profile (VSP) surveys. Independently of the medium above the geophone (homogeneous or heterogeneous) and the shape of the well (directional or curved, vertical or sloped), an inversion is performed from a first-order approximation around a reference isotropic medium. The analysis of the inversion scheme considers factors such as the noise level of the data, the type of P-wave, the degree of the anisotropy of the medium, the choice of parameters in the reference isotropic medium and the degree of heterogeneity of the medium.

Keywords: anisotropy estimation, multi-azimuth walkaway VSP data, weak anisotropy.

RESUMO. Neste trabalho é apresentada uma análise do esquema de inversão linear para a estimativa de anisotropia na vizinhança de um receptor situado em um poço a partir da componente vertical do vetor de vagariedade e do vetor de polarização das ondas P medidos em experimentos de VSP *walkaway* multiazimutal. Independente do meio acima do geofone (homogêneo ou heterogêneo) e da geometria do poço (inclinado, reto ou curvo), a inversão é feita a partir de uma aproximação de primeira ordem em torno de um meio isotrópico de referência. O esquema de inversão é analisado considerando diferentes fatores, tais como: nível de ruído nos dados, tipo de onda P, grau de anisotropia do meio, escolha dos parâmetros no meio isotrópico de referência e grau de heterogeneidade do meio.

Palavras-chave: estimativa de anisotropia local, dados de VSP *walkaway* multiazimutal, fraca anisotropia.

INTRODUCTION

A large number of hydrocarbon reservoirs are fractured and, in near-static regimes, behave as anisotropic media (Schoenberg & Douma, 1988). This has raised general interest within companies and the academic community in studying anisotropy. Using information about the medium's anisotropy parameters, one can determine, for example, the preferred flow direction within the reservoir.

In studies such as Horne & Leaney (2000); Zheng & Pšenčík (2002); Gomes et al. (2004); Rusmanugroho & McMechan (2012); and Barreto et al. (2013), the anisotropic parameters of a medium are estimated by inversion of P-wave (or P- and S-wave) slowness and polarization data measured in vertical seismic profile (VSP) surveys.

The relationship between the anisotropic parameters of a medium and its slowness and polarization data are complex. Zheng & Pšenčík (2002) used only P-wave data to produce a linear approximation around a reference isotropic medium that correlated slowness and polarization data to weak anisotropy (WA) parameters of the medium (Farra & Pšenčík, 2003). Using this methodology and considering only the vertical component of the P-waves' slowness and polarization vectors from a single VSP profile, Gomes et al. (2004) estimated the anisotropy using data from a region of the Java Sea. Barreto et al. (2013) estimated the anisotropy by studying the experimental design of multi-azimuth walkaway VSP surveys. This inversion scheme does not depend on the structure of the medium above the geophone (it can be homogeneous or heterogeneous), nor does it depend on the shape of the well (it can be directional or curved, vertical or sloped). In this study, the authors analyze the dependence of this inversion scheme on factors such as the degree of anisotropy, the noise level of the slowness and polarization data, the type of wave used (direct and/or reflected P-waves), the choice of anisotropic parameters for the medium and its degree of heterogeneity. This provides continuation for the analysis presented in Barreto et al. (2013). A similar analysis can be found in Rusmanugroho & McMechan (2012); however, this work differs from the Rusmanugroho's study both methodology and the type of wave used in the inversion.

The tests presented here used synthetic slowness and polarization data that were generated using the ANRAY package (Gajewski & Pšenčík, 1990). Throughout this article, matrices and vectors are represented by boldface upper- and lowercase letters, respectively. Index notation and the summation convention are used throughout the text (Aki & Richards, 1980). Exceptions to these rules are explicitly noted.

METHODOLOGY

The direct model

This problem uses a Cartesian coordinate system (x, y, z) with the positive z -axis pointing downwards. From Zheng & Pšenčík, 2002 (Eq. 22) gives the relationship between the vertical component of slowness, the polarization vector and the weak anisotropy parameters for a receiver inside a well:

$$D(\alpha^2 - \beta^2)B_{13} - \frac{1}{2}\alpha^{-1}\eta B_{33} = Dg_i e_i^{(1)} + \alpha\Delta\eta, \quad (1)$$

where

$$D = \sqrt{n_1^2 + n_2^2}, \eta = \alpha^{-1}n_3. \quad (2)$$

The symbols α and β denote, respectively, the velocities of P- and S-waves in the reference isotropic medium. Vector $\mathbf{n} = (n_1, n_2, n_3)$ in Eq. (2) is the unit vector perpendicular to the P-wave front in the reference isotropic medium. Vector $\mathbf{e}^{(1)}$ is a unit vector perpendicular to \mathbf{n} . Vectors $\mathbf{e}^{(1)}$ and $\mathbf{n} = \mathbf{e}^{(3)}$ are confined to the vertical plane that contains the profile being studied. They are part of the vector system that comprises $\mathbf{e}^{(1)}$, $\mathbf{e}^{(2)}$ and $\mathbf{e}^{(3)}$ in the reference medium and are chosen as follows (Pšenčík & Gajewski, 1998):

$$\begin{aligned} \mathbf{e}^{(1)} &= D^{-1}(n_1 n_3, n_2 n_3, n_3^2 - 1); \\ \mathbf{e}^{(2)} &= D^{-1}(-n_2, n_1, 0); \\ \mathbf{e}^{(3)} &= D^{-1}(n_1, n_2, n_3); \end{aligned} \quad (3)$$

In Equation (1), g_i and the quantity $\Delta\eta = p_3^{\text{obs}} - \eta$ are the observed data and correspond to the i -th component of the polarization vector and the difference between the vertical components of the slowness vectors in the anisotropic and reference isotropic media, respectively. Matrices \mathbf{B}_{13} and \mathbf{B}_{33} , which are of the form \mathbf{B}_{mn} with $m, n = 1, 2, 3$, are weak anisotropy matrices projected in the directions of the $\mathbf{e}^{(k)}$ vectors:

$$\mathbf{B}_{mn} = a_{ijkl} e_i^{(m)} e_j^{(3)} e_k^{(3)} e_l^{(n)} - \alpha^2 \delta_{mn}, \quad (4)$$

where a_{ijkl} is the tensor containing density-normalized elastic parameters, and $i, j, k, l = 1, 2, 3$. The weak anisotropy matrix \mathbf{B}_{mn} (with $m, n = 1, 2, 3$) corresponds to the first-order perturbation of the Christoffel matrix around the reference isotropic medium (Pšenčík & Gajewski, 1998). The vertical component of the slowness and the P-wave polarization vector used in the inversion depend solely on matrices \mathbf{B}_{13} and \mathbf{B}_{33} of \mathbf{B}_{mn} . For an arbitrary anisotropic medium, these matrices can be written as (Pšenčík & Gajewski, 1998):

$$\mathbf{B}_{13} = \alpha D^{-1} \left\{ 2\varepsilon_z n_3^5 + n_3^4 + n_3^4 (\varepsilon_{34} n_2 + \varepsilon_{35} n_1) + n_3^3 (\delta_x n_1^2 + \delta_y n_2^2 + 2\chi_z n_1 n_2 - 2\varepsilon_z) \right. \\ \left. + n_3^2 [(4\chi_x - 3\varepsilon_{34}) n_1^2 n_2 + (4\chi_y - 3\varepsilon_{35}) n_1 n_2^2 + (4\varepsilon_{15} - 3\varepsilon_{35}) n_1^3 + (4\varepsilon_{24} - 3\varepsilon_{34}) n_2^3] \right. \\ \left. + n_3 [(2\delta_z - \delta_x - \delta_y) n_1^2 n_2^2 + 2(2\varepsilon_{16} - \chi_z) n_1^3 n_2 + (2\varepsilon_{26} - \chi_z) n_1 n_2^3] \right. \\ \left. + (2\varepsilon_x - \delta_x) n_1^4 + (2\varepsilon_y - \delta_y) n_2^4 - \chi_x n_2^2 n_2 - \chi_y n_1 n_2^2 - \varepsilon_{15} n_1^3 - \varepsilon_{24} n_2^3 \right\}, \quad (5)$$

$$\mathbf{B}_{33} = 2\alpha^2 \left\{ \varepsilon_z n_3^4 + 2n_3^3 (\varepsilon_{34} n_2 + \varepsilon_{35} n_1) + n_3^2 (\delta_x n_1^2 + \delta_y n_2^2 + 2\chi_z n_1 n_2) \right. \\ \left. + 2n_3 (\chi_x n_1^2 n_2 + \chi_y n_1 n_2^2 + \varepsilon_{15} n_1^3 + \varepsilon_{24} n_2^3) + \varepsilon_x n_1^4 + \delta_z n_2^2 n_2^2 \right. \\ \left. + \varepsilon_y n_2^4 + 2\varepsilon_{16} n_1^3 n_2 + 2\varepsilon_{26} n_1 n_2^3 \right\}. \quad (6)$$

Parameters ε , δ and χ are called the weak anisotropy (WA) parameters; their definition is given in Pšenčík & Gajewski (1998); they are a natural generalization of the parameters introduced by Thomsen (1986). Parameter ε follows the notation given in Pšenčík & Gajewski (1998). Matrices \mathbf{B}_{13} and \mathbf{B}_{33} depend on α , β , the vector \mathbf{n} and the WA parameters.

Sensitivity matrix

Eq. (1) can be written in matrix form, i.e.,

$$\mathbf{M}\mathbf{x} = \mathbf{y}, \quad (7)$$

where the vector \mathbf{y} is dimensionless and is related to the observed data (the right-hand side of Eq. (1) for each source-receiver pair) and has size equal to the number of observations, N_{obs} . The vector \mathbf{x} is related to the WA parameters and has size equal to the number of parameters, N_{par} . Only 15 WA parameters control the P-wave propagation, namely:

$$\begin{aligned} x_1 &= \varepsilon_x & x_2 &= \varepsilon_y & x_3 &= \varepsilon_z \\ x_4 &= \delta_x & x_5 &= \delta_y & x_6 &= \delta_z \\ x_7 &= \chi_x & x_8 &= \chi_y & x_9 &= \chi_z \\ x_{10} &= \varepsilon_{15} & x_{11} &= \varepsilon_{16} & x_{12} &= \varepsilon_{24} \\ x_{13} &= \varepsilon_{26} & x_{14} &= \varepsilon_{34} & x_{15} &= \varepsilon_{35} \end{aligned} \quad (8)$$

These WA parameters are related to the normalized elastic parameters as follows:

$$\begin{aligned} \varepsilon_x &= \frac{A_{11} - \alpha^2}{2\alpha^2}, & \varepsilon_y &= \frac{A_{22} - \alpha^2}{2\alpha^2}, & \varepsilon_z &= \frac{A_{33} - \alpha^2}{2\alpha^2}, \\ \delta_x &= \frac{A_{13} + 2A_{55} - \alpha^2}{\alpha^2}, & \delta_y &= \frac{A_{23} + 2A_{44} - \alpha^2}{\alpha^2}, & \delta_z &= \frac{A_{12} + 2A_{66} - \alpha^2}{\alpha^2}, \\ \chi_x &= \frac{A_{14} + 2A_{56}}{\alpha^2}, & \chi_y &= \frac{A_{25} + 2A_{46}}{\alpha^2}, & \chi_z &= \frac{A_{36} + 2A_{45}}{\alpha^2}, \\ \varepsilon_{15} &= \frac{A_{15}}{\alpha^2}, & \varepsilon_{16} &= \frac{A_{16}}{\alpha^2}, & \varepsilon_{24} &= \frac{A_{24}}{\alpha^2}, \\ \varepsilon_{26} &= \frac{A_{26}}{\alpha^2}, & \varepsilon_{34} &= \frac{A_{34}}{\alpha^2}, & \varepsilon_{35} &= \frac{A_{35}}{\alpha^2}. \end{aligned} \quad (9)$$

In Eq. (1), the density-normalized elastic parameters a_{ijkl} are in their reduced representation A_{ij} (Helbig, 1994). In Eq. (7), the matrix $\mathbf{M}(\alpha, \beta, \mathbf{n})$, which corresponds to the left-hand side of Eq. (1), is called the sensitivity matrix (see appendix for details) and has size $N_{\text{obs}} \times N_{\text{par}}$ (the number of observations \times the number of parameters). The sensitivity matrix depends on the geometry of acquisition, the number and orientation of the profiles on the surface on which the sources of the multi-azimuth walkaway VSP survey are distributed (Fig. 1) and the parameters of the reference isotropic medium.

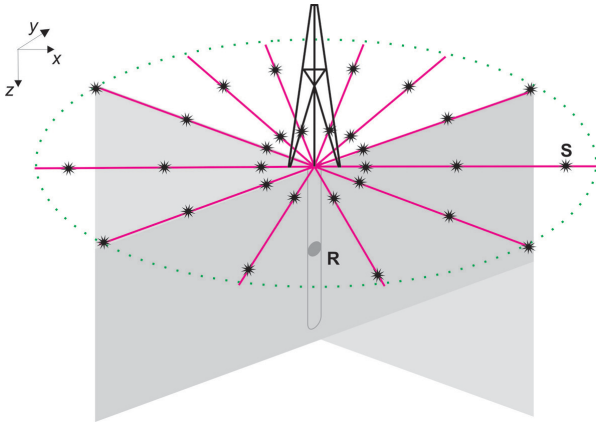


Figure 1 – Configuration of the multi-azimuth VSP acquisition. Sources (S, in black) are located along profiles (in magenta) on the surface at each side of the well, which is in the center. Receivers are located inside the well.

This dependency is analyzed in detail in Barreto et al. (2013), where it is shown that to uniquely estimate the 15 WA parameters, the surface sources must be distributed on both sides of the well in at least five regularly spaced profiles. In this study, the data were acquired in six regularly spaced profiles spanning 0° to 360° and spaced by 36° .

The inverse problem

The WA parameters can be estimated from Eq. (7) by determining which values of the vector x_j minimize the function

$$\Phi = \sum_{i=1}^{N_{\text{obs}}} (y_i - M_{ij} \tilde{x}_j). \quad (10)$$

The M_{ij} are the elements of the sensitivity matrix \mathbf{M} , \tilde{x}_j are WA parameter estimates and y_i is the i -th component of the observation vector \mathbf{y} . In this work, the observation vector is synthetically generated using the ANRAY package for ray tracing in anisotropic media (Pšenčík & Gajewski, 1998).

To analyze the stability of the WA parameter estimates, a unique Gaussian noise signal was added to each synthetic ob-

servation. The velocities α and β and WA parameters were estimated from these noisy observations. The mean and the standard deviation of these estimates were calculated as follows:

$$\bar{x}_j = \frac{\sum_{k=1}^{N_s} \tilde{x}_j^k}{N_s} \quad (11)$$

$$\bar{v}_j = \sqrt{\frac{\sum_{k=1}^{N_s} (\tilde{x}_j^k)^2}{N_s} - [N_s \bar{x}_j]^2} \quad (12)$$

Here, N_s is the number of simulations ($N_s = 500$), the index j refers to the number of WA parameters ($j = 1, K, 15$), and \bar{x}_j and \bar{v}_j are the sample mean and standard deviation of the estimates for the \tilde{x}_j parameters, respectively.

To perform the inversion, the matrix $\mathbf{M}(\alpha, \beta, \mathbf{n})$ must be known; therefore, it is necessary that the reference isotropic medium's parameters (P- and S-wave velocities and \mathbf{n} , the normal vector of the P-wave front) be known. The many ways to determine these parameters are presented in Barreto et al. (2013). In this study, the reference isotropic medium's parameters were chosen based solely on the observed data. Thus, the P-wave velocity in the reference isotropic medium is given by

$$\alpha p_3^{(i)} = g_3^{(i)}, \quad (13)$$

where $p_3^{(i)}$ and $g_3^{(i)}$ are the vertical components of the slowness and polarization vectors generated by the i -th observation, respectively. The velocity α in the reference medium can then be estimated by inverting Equation (13) using least squares on the total number of observations N_{obs} . The S-wave velocity in the reference isotropic medium, β , is given by the Poisson ratio for sedimentary medium:

$$\beta = \frac{\alpha}{\sqrt{3}}. \quad (14)$$

The normal vector of the P-wave front in the reference isotropic medium was determined by the relation $\mathbf{n} // \mathbf{g}$. When weakly anisotropic media are considered, this equation gives a good estimate for \mathbf{n} . A consequence this relation is that $g_i e_i^{(1)} = 0$, which makes the first term of the right-hand side of Eq. (1) vanish.

Thus, the estimates of WA parameters in Eq. (7) are obtained by inverting Eq. (10) using singular value decomposition. Inversion stabilizers were not used because the condition number of the sensitivity matrices of tests performed herein was of the order of 10^2 , which indicates that the problem is well posed.

Experimental configuration and models

Numerical tests were performed according to two models that differ in their degree of anisotropy (as established by Thomsen,

1986) and the geometry of acquisition. In Model I, the configuration used in data acquisition is multi-azimuth walkaway VSP (Fig. 1), with 18 sources per profile, located on the surface and spaced by 0.1 km (Fig. 2). Data were measured over six profiles spaced at regular 36° intervals.

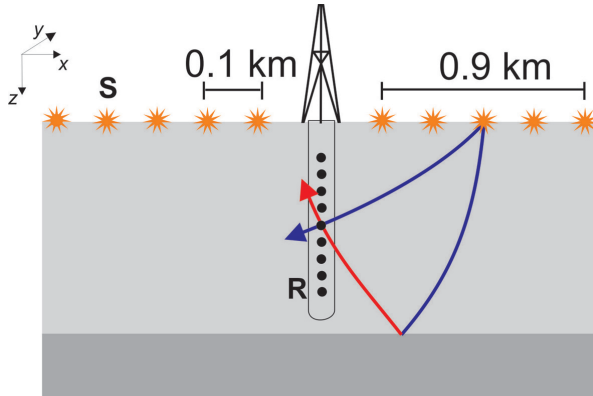


Figure 2 – Placement of sources and receivers for Model I, where sources (S) are spaced by 0.1 km on the surface, the well is in the center, and the receivers (R) are inside the well. Direct and indirect P-waves are shown in blue and red, respectively.

The model contains two layers. The top of the first layer was initially in a VTI medium (isotropic medium with a vertical symmetry axis) with the following density-normalized elastic parameters (N/m²): $A_{11} = A_{22} = 15.71$, $A_{33} = 13.39$, $A_{12} = 5.05$, $A_{13} = A_{23} = 4.46$, $A_{44} = A_{55} = 4.98$ and $A_{66} = 5.33$. The medium's symmetry axis was rotated by $\theta = 80^\circ$ around the y -axis and then by $\varphi = 25^\circ$ around the z -axis (making the model at the top, therefore, into a TI). The bottom of the first layer, located at a depth of 5 km, was initially a VTI with the following density-normalized elastic parameters (N/m²): $A_{11} = A_{22} = 35.348$, $A_{33} = 30.128$, $A_{12} = 11.363$, $A_{13} = A_{23} = 10.035$, $A_{44} = A_{55} = 11.205$ and $A_{66} = 11.992$. The medium's symmetry axis was rotated by $\theta = 90^\circ$ around the y -axis (making the model at the bottom, therefore, into a HTI, i.e., an isotropic medium with a horizontal symmetry axis). This makes the first layer an anisotropic medium, and using the common measure for P-wave anisotropy (maximum $\varepsilon \times 100\%$, where ε represents ε_x , ε_y or ε_z), the model's anisotropy in the layer is 8%. The second layer is isotropic, with density-normalized P- and S-wave velocities $\alpha = 4.0$ km/s and $\beta = 2.35$ km/s, respectively, and is 1 km thick.

In Model II, the configuration used in data acquisition is 60 sources distributed along six profiles on the surface, the azimuths of which vary between 0° and 360° at 30° increments (Fig. 3). The sources are spaced so that the inclinations of the direct ray from front to the receiver vary between -75° and 75°, with an increment of 0.25 km (Fig. 4) in relation to the vertical axis.

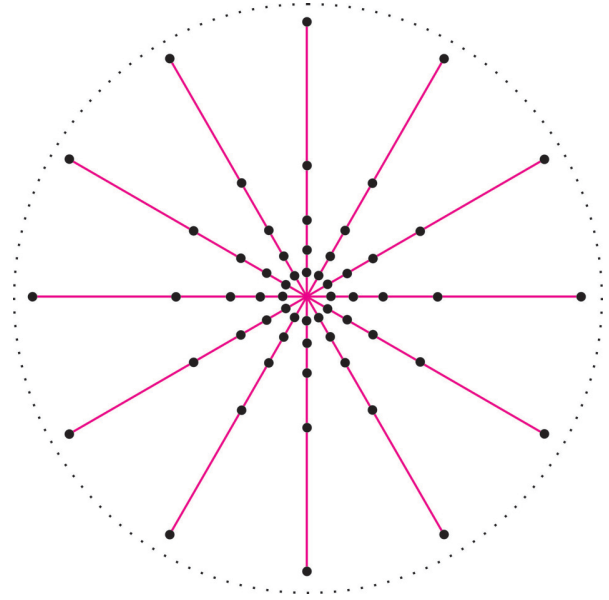


Figure 3 – Profile distribution (magenta) for Model II, where black dots represent sources and the well head is in the center.

This model consists of two plane layers, where the first layer (the incident medium) is a homogeneous triclinic anisotropic medium of 1.1 km thickness, as presented in Rusmanugroho & McMechan (2012). The density-normalized elastic parameter tensor, in N/m², has the following values:

$$A_{ij} = \begin{bmatrix} 5.562 & 2.192 & 2.598 & 0.149 & -0.015 & -0.331 \\ & 5.515 & 2.609 & 0.207 & -0.009 & -0.290 \\ & & 6.789 & 0.216 & -0.014 & -0.224 \\ & & & 1.764 & -0.066 & -0.001 \\ & & & & 1.749 & 0.039 \\ & & & & & 1.658 \end{bmatrix} \quad (15)$$

The degree of anisotropy in the first layer is 10%; thus, this layer is considered moderately anisotropic (Thomsen, 1986).

The second layer, which is 0.9 km thick, is an isotropic medium for which the density-normalized P- and S-wave velocities are given by the square roots of the incident medium's A_{33} and A_{44} , respectively.

NUMERICAL TESTS

Numerical tests that are, in fact, the continuity to the work presented in Barreto et al. (2013), are presented. These tests analyze how WA parameter estimates depend on the noise level of the slowness and polarization data, the type of anisotropy in the model and the type of P-wave used in the inversion.

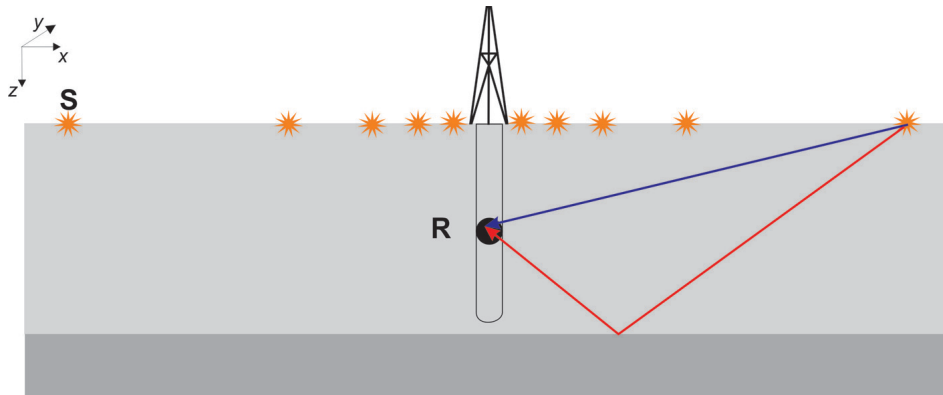


Figure 4 – A homogeneous medium in which sources are irregularly distributed. The blue line represents the direct wave and the red line represents the reflected wave. Both lines are straight because the medium is homogeneous.

Noise level

Various levels of noise were added to the slowness and polarization data of Model I. The noise added to the vertical components of the slowness vectors had standard deviation equal to a percentage of the largest value observed for the vertical component of that slowness vector. For the polarization data, the noise was related to changes in the direction of polarization. Four levels of noise were used:

- I. Noise level I. For polarization data: 1° (direct waves) and 2° (reflected waves). For slowness data: 5% (direct waves) and 10% (reflected waves). This noise level will be referred to as the reference noise level.
- II. Noise level II. For polarization data: 1° (direct waves) and 2° (reflected waves). For slowness data: 10% (direct waves) and 20% (reflected waves).
- III. Noise level III. For polarization data: 2° (direct waves) and 4° (reflected waves). For slowness data: 5% (direct waves) and 10% (reflected waves).
- IV. Noise level IV. For polarization data: 2° (direct waves) and 4° (reflected waves). For slowness data: 10% (direct waves) and 20% (reflected waves).

The results from estimating the WA parameters through inversion were analyzed by comparing stereographic projections of the first-order approximation for the phase velocity (Pšenčík & Gajewski, 1998) given by the exact and estimated WA parameter values. The first-order formula for the phase velocity is

$$\mathbf{c}^2(x_m, n_m) = \sqrt{\alpha^2 + \mathbf{B}_{33}}. \quad (16)$$

Phase velocity $c(x_m, n_m)$ is a function of the vector $\mathbf{n} = (n_1, n_2, n_3)$ and the parameter vector \mathbf{x} (see Eq. (7) for definitions). Four types of stereographic projections are shown: a) squared phase velocity computed from the exact WA parameters; b) squared phase velocity computed from the estimated WA parameters; c) error percentile between b) and a); d) variation percentile of the estimated phase velocity.

Tests were performed using slowness and polarization data measured by two receivers inside the well: a shallower one at 0.1 km (Receiver #1) and a deeper one at 0.7 km (Receiver #2). Figure 5 shows the phase velocity stereograms computed from the exact WA parameters (Fig. 5a) and for the four noise levels (Figs. 5b, 5d, 5f and 5h) and the respective relative errors (Figs. 5c, 5e, 5g and 5i).

Phase velocity variation was also computed for Receiver #1. The stereograms in Figure 6 represent the phase velocity variations computed from Eq. (17) using the WA parameters estimated from the 500 inversions based on noise level I data (Fig. 6a), noise level II data (Fig. 6b), noise level III data (Fig. 6c) and noise level IV data (Fig. 6d).

Results for the deeper receiver are shown in Figures 7 and 8. Figure 7 shows the phase velocity stereograms computed from the exact WA parameters (Fig. 7a) and for the four noise levels (Figs. 7b, 7d, 7f and 7h), along with the respective relative errors (Figs. 7c, 7e, 7g and 7i). The variation in phase velocity was similarly computed from the WA parameters estimated at the four noise levels, and shown in Figure 8.

As in Figure 6, the variations shown in the stereograms of Figure 8 were obtained from the phase velocity computed using Eq. (17) and the parameters estimated from the 500 inversions based on data with the four levels (I through IV) of noise added, corresponding to Figures 8a through 8d.

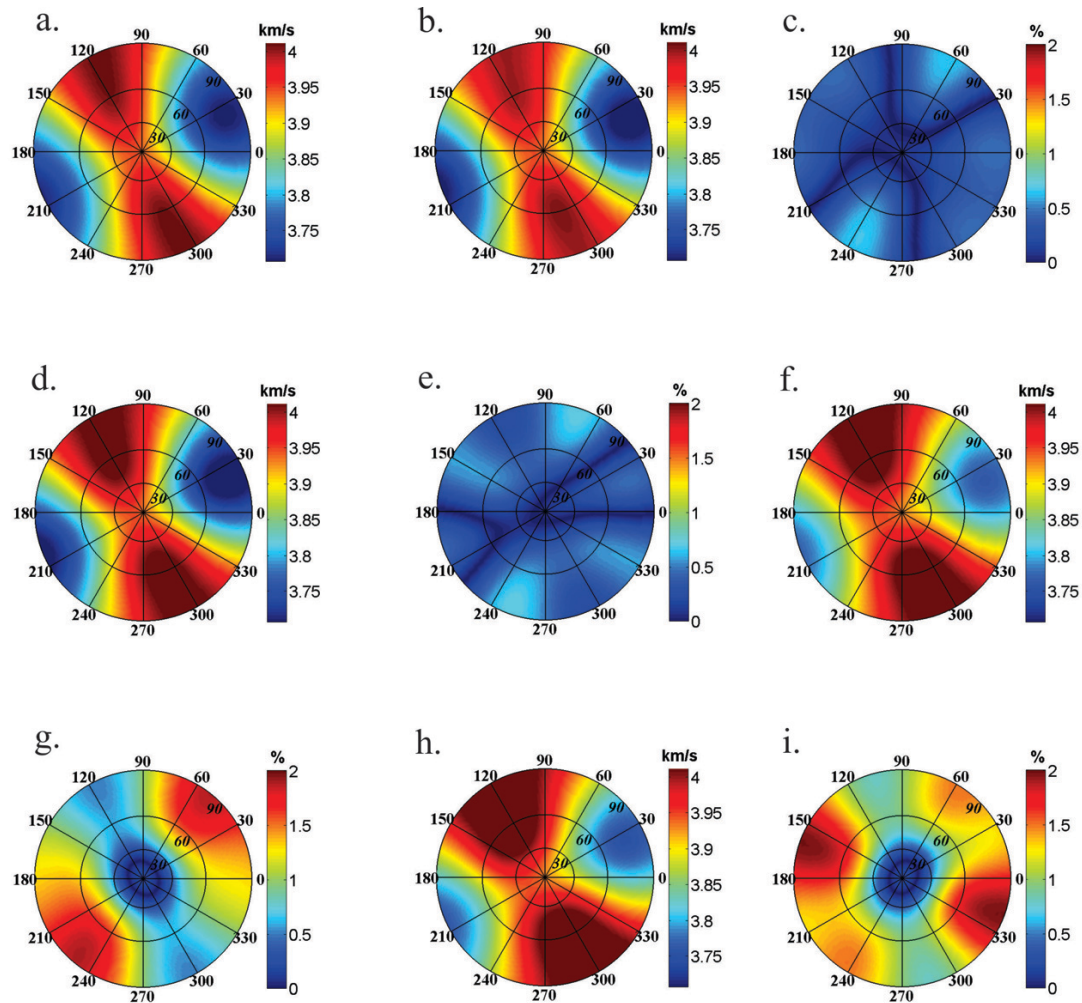


Figure 5 – For Receiver #1 in Model I (the shallower receiver), the stereograms represent a) the phase velocity computed using the WA parameters; b) the phase velocity computed using the WA parameters estimated from slowness and polarization data with level I noise; c) the relative error percentile between phase velocities in (a) and (b); d) the phase velocity computed using the WA parameters estimated from slowness and polarization data with level II noise; e) the relative error percentile between phase velocities in (a) and (d); f) the phase velocity computed using the WA parameters estimated from slowness and polarization data with level III noise; g) the relative error percentile between phase velocities in (a) and (f); h) the phase velocity computed using the WA parameters estimated from slowness and polarization data with level IV noise; i) the relative error percentile between phase velocities in (a) and (h).

From the phase velocity results presented in Figures 5 through 8, when the WA parameter estimates vary with to the level of noise, one can conclude the following:

- The stability of the estimates is more sensitive to noise in the slowness data than to noise in the polarization data. However, increasing the noise in the polarization data does worsen the WA parameter estimate values.
- WA parameter estimates are generally more sensitive (with respect to stability and the accuracy of the estimated values) to the polarization data than to the slowness data. This is expected because, in choosing the reference isotropic medium's parameters, the vector normal to the P-wave

front was taken as parallel to the observed polarization vector. Therefore, not only are the data on the right-hand side of Eq. (7) noisy, but the sensitivity matrix \mathbf{M} itself is also noisy.

- Estimates oscillate more at Receiver #2, at greater depth, than at Receiver #1, nearer to the surface. It is believed this is due to reduced coverage.
- Given that the degree of anisotropy of the model used in the tests is 8%, it is assumed that the best estimates should display variation of no more than approximately 4%. In this case, the best results are those obtained with

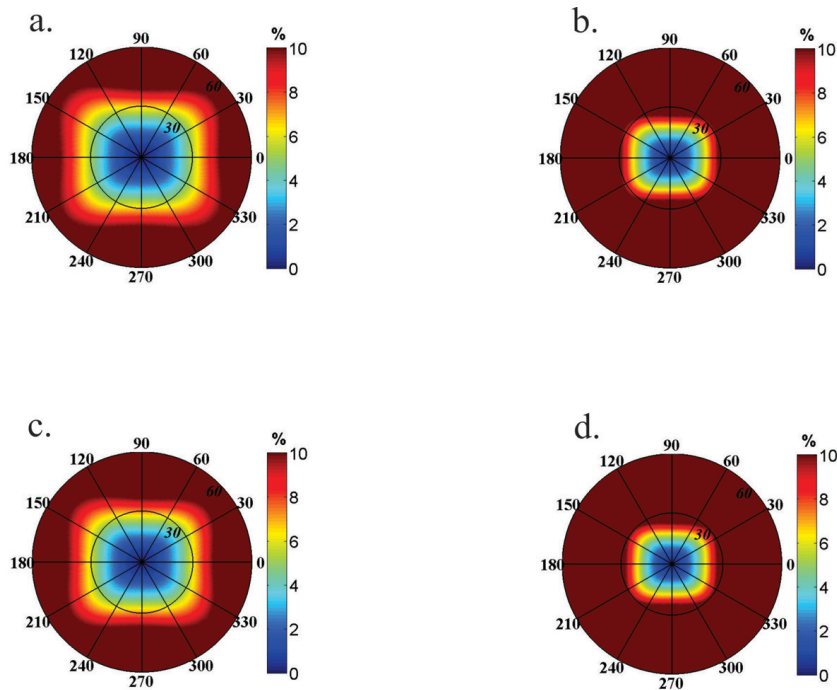


Figure 6 – Stereograms showing the percent variation of the phase velocity in all directions for Receiver #1 in Model I.

level I noise, i.e., the noise added to the polarization data changes their direction by 1° (for direct waves) and 2° (for reflected waves), and the noise added to the vertical component of the slowness data has standard deviation of 5% (for direct waves) and 10% (for reflected waves) of the maximum observed value. This noise level is referred to as the reference noise level.

- For the reference noise level, seven of the fifteen WA parameters that describe the P-wave propagation are well estimated; these are ε_z , χ_x , χ_y , ε_{15} , ε_{24} , ε_{34} and ε_{35} .
- It can be seen in the estimated variation stereograms that the seven WA parameters are well estimated where the geophones for the reference noise level are placed, within a 30° cone around the well.

Degree of anisotropy

Tests at various degrees of anisotropy were performed. The results for the inversion of Model II with moderate anisotropy (approximately 10%, Thomsen, 1986) are presented in Figures 9 and 10. Figure 9 shows the values for the phase velocity calculated with the exact WA parameters (Fig. 9a) and calculated using the WA parameters estimated from inverting slowness and polarization data for the different noise levels (Figs. 9b, 9d, 9f and 9h); it also shows the relative error percentages (Figs. 9c, 9e, 9g and 9i). Figure 10

shows the variations observed in the stereograms obtained from the phase velocity computed using Eq. (17) and the parameters estimated from the 500 inversions based on data containing the four noise levels I through IV (Figs. 10a through 10d).

Inspection of Figures 9 and 10 shows that estimates for the model with a moderate degree of anisotropy have larger errors and variations than the results obtained for Model I, which has weak anisotropy. This is because the inversion scheme used in this work is based on an approximation around an isotropic reference medium. Therefore, the weaker the anisotropy of the medium is, the better the result from the inversion is expected to be.

The previous observations of the results of Model I hold for the moderate anisotropy case of Model II: the stability of estimates is more sensitive to noise in the slowness data than to noise in the polarization data, although increasing the latter does worse the estimated WA parameter values.

Wave type

The WA parameters were then estimated at Receiver #1 of Model I using either only direct P-wave data or direct and reflected P-wave data. The reference noise (5% of the maximum value of the vertical component of slowness and a polarization error of 1°) was used in the direct P-wave polarization and slowness data; twice this amount of noise was applied to the reflected wave data.

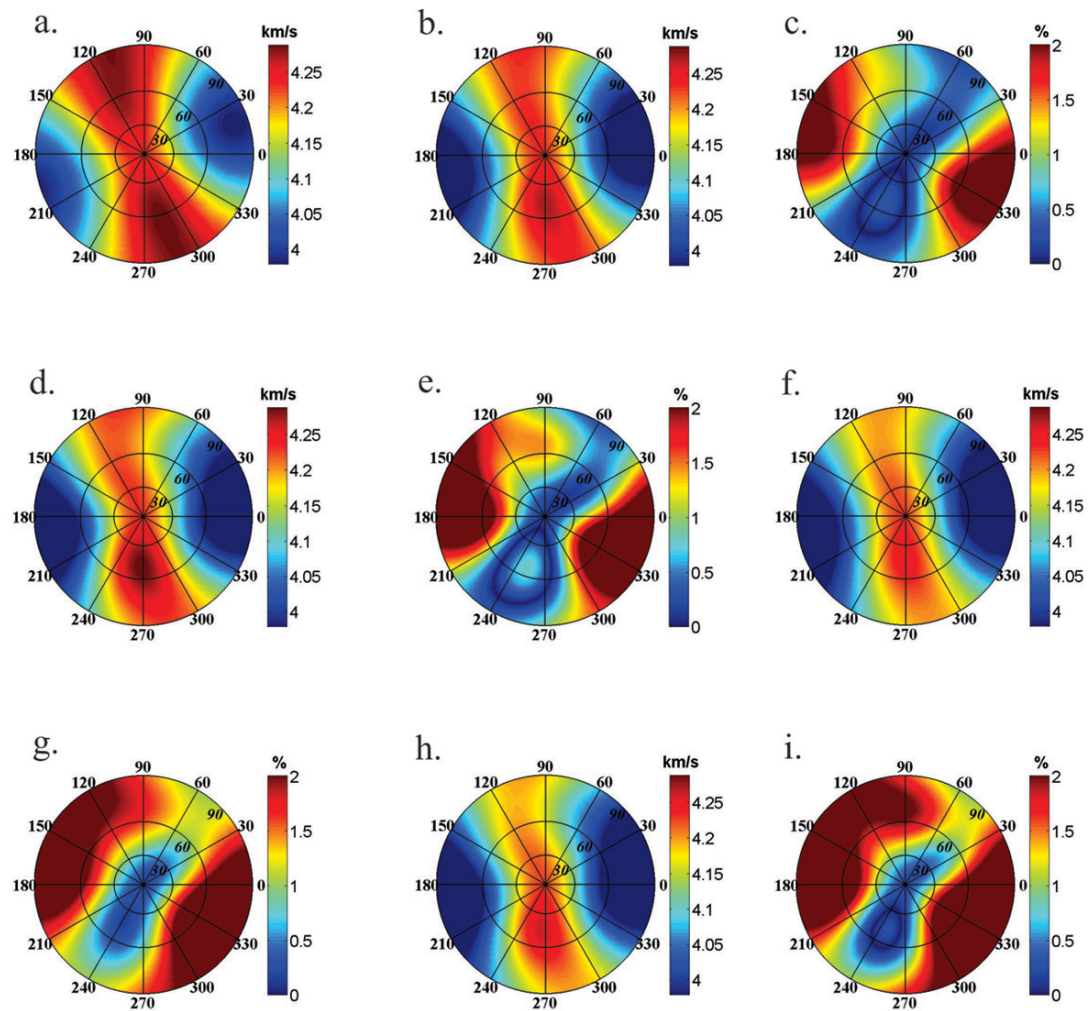


Figure 7 – For Receiver #2 in Model I (the deeper receiver), the stereograms represent a) the phase velocity computed using the WA parameters; b) the phase velocity computed using the WA parameters estimated from slowness and polarization data with level I noise; c) the relative error percentile between phase velocities in (a) and (b); d) the phase velocity computed using the WA parameters estimated from slowness and polarization data with level II noise; e) the relative error percentile between phase velocities in (a) and (d); f) the phase velocity computed using the WA parameters estimated from slowness and polarization data with level III noise; g) the relative error percentile between phase velocities in (a) and (f); h) the phase velocity computed using the WA parameters estimated from slowness and polarization data with level IV noise; i) the relative error percentile between phase velocities in (a) and (h).

Figure 11 shows, for Receiver #1, the percentage error between the exact phase velocity and the velocity computed using the WA parameter estimates obtained by inverting direct and reflected wave data (Fig. 11a) and that computed using the WA parameter estimates obtained by inverting only direct wave data (Fig. 11b).

As can be seen in Figure 11, the best estimate is obtained when both direct and reflected P-waves are considered, even if the noise associated with the reflected waves is twice that of the direct waves. It is believed that this is because more information is used in the inversion. When only direct waves are used, the error in estimates is approximately 2.5 times larger than the error obtained when both direct and reflected P-wave data are used, and

larger variations in estimates are also observed when only direct P-wave data are used.

CONCLUSION

This study presents the analysis of an inversion scheme for a medium's weak anisotropy (WA) parameters from P-wave polarization and slowness data in a multi-azimuth VSP survey for the estimation of local anisotropy. The relationship between the medium's parameters and the observed VSP data is a first-order approximation around an isotropic reference medium, as presented in Zheng & Pšenčík (2002). This inversion scheme is

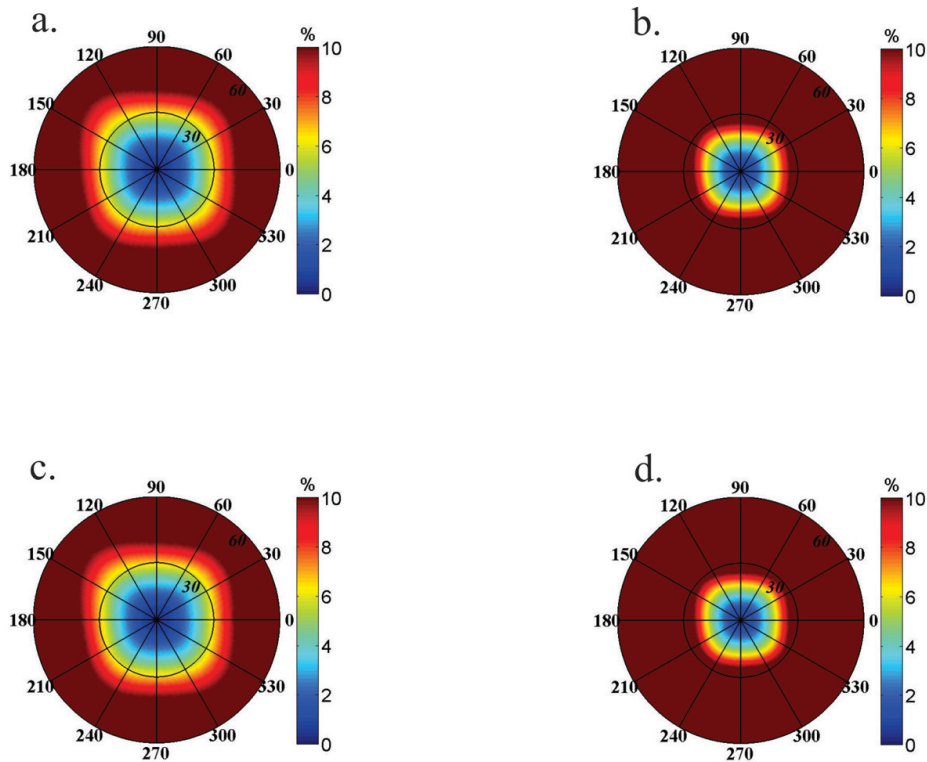


Figure 8 – Stereograms showing the percent variation of the phase velocity in all directions for Receiver #2 in Model I.

affected by factors such as the amount of noise in the data, the orientation of the well, the type of seismic wave, the degree of anisotropy and the choice of parameters for the isotropic reference medium. This work provides an analysis of how these factors influence the estimation of WA parameters.

According to the analyses performed herein, the following can be concluded:

- By considering both slowness and polarization data containing different levels of noise, it has been verified that WA parameters can be estimated when moderate noise is present. Only seven of the fifteen WA parameters that describe the P-wave propagation are estimated. The estimates of the WA parameters are evaluated by computing the phase velocity; estimating the phase velocity is useful in constructing velocity models applicable to seismic imaging, where vertical velocities are not easily estimated from surface data.
- According to computational tests based on data measured along six regularly spaced profiles, the WA parameters and P-wave phase velocities are well estimated inside a 30° cone around the receiver placed inside the well. This is most likely because the accuracy of the estimate depends

on the data coverage. Because the data used in the inversion are the components of the slowness vector along the local orientation of the well, the most reliable estimates are found in a cone for which the axis coincides with that orientation. As a consequence, only the WA parameters affecting these data are well resolved. Therefore, the parameter ε_z , which is related to the elastic parameter c_{33} , is the best-estimated parameter, and the reference isotropic medium is thus well estimated. Moreover, for incidences less than 30° , the phase velocity approaches the velocity of the reference medium and depends only on the WA parameter subset $\varepsilon_z, \chi_x, \chi_y, \varepsilon_{15}, \varepsilon_{24}, \varepsilon_{34}$ and ε_{35} , the parameters which are best resolved in this inversion scheme.

- By comparing the inversion using only direct P-wave data to the inversion using both direct and reflected P-wave data, it was observed that WA parameter estimation using only direct wave data had lower resolution and stability than if an inversion using both direct and reflected wave data. Similarly, the estimate obtained from inverting only reflected wave data is poorer than the result using both data.

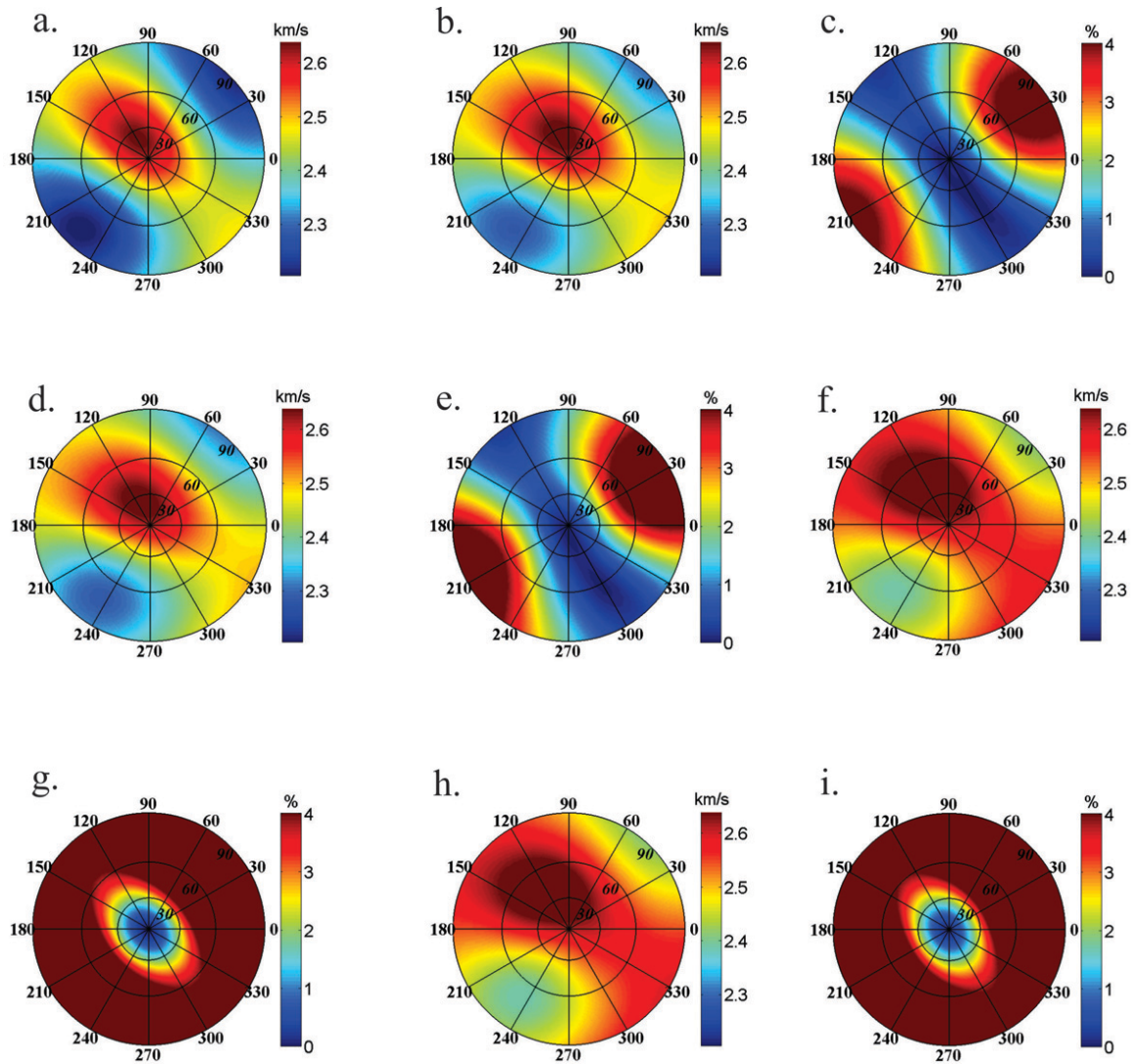


Figure 9 – For a receiver at a depth of 0.25 km in Model II, the stereograms represent a) the phase velocity computed using the WA parameters; b) the phase velocity computed using the WA parameters estimated from slowness and polarization data with level I noise; c) the relative error percentile between phase velocities in (a) and (b); d) the phase velocity computed using the WA parameters estimated from slowness and polarization data with level II noise; e) the relative error percentile between phase velocities in (a) and (d); f) the phase velocity computed using the WA parameters estimated from slowness and polarization data with level III noise; g) the relative error percentile between phase velocities in (a) and (f); h) the phase velocity computed using the WA parameters estimated from slowness and polarization data with level IV noise; i) the relative error percentile between phase velocities in (a) and (h).

- When models with different degrees of anisotropy were considered, estimation of WA parameters was performed by inverting Eq. (1), which is a linear approximation around an arbitrary isotropic medium; therefore, media with lower degrees of anisotropy will have better performances and results. For media with moderate to strong anisotropy (20%), it was observed that this inversion scheme fails.

Tests that considered other choices for the isotropic reference medium's parameters and degree of heterogeneity were also

performed to estimate the WA parameters. These tests led to the following conclusions:

- There are three possible choices for the P-wave front normal vector (\mathbf{n}_k) in the reference medium. These three choices do not significantly affect the estimation of the WA parameters as long as the medium is homogeneous or weakly heterogeneous. In the tests conducted in the present study, heterogeneity did not exceed 30% and was constrained to the vertical direction. All synthetic tests for the estimation of the WA parameters using

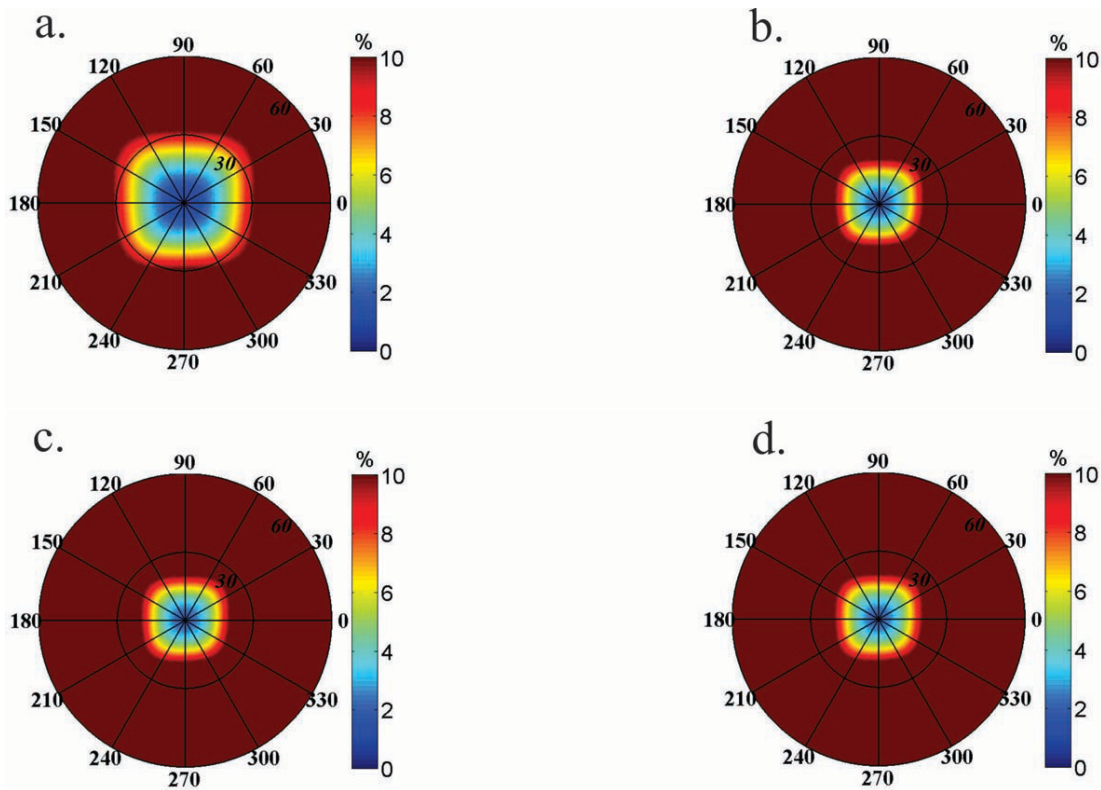


Figure 10 – Stereograms showing the percent variation of the phase velocity in all directions for Model II.

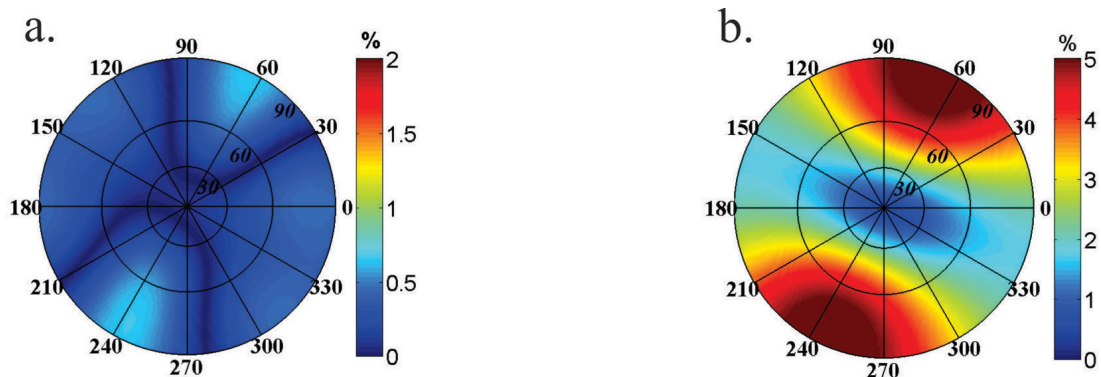


Figure 11 – Stereograms representing the error in the phase velocity computed using the WA parameters estimated from: a) direct and reflected P-wave polarization and slowness data, and b) only direct P-wave polarization and slowness data.

models with weak anisotropy determined the angle between the \mathbf{n}_k vector within the reference medium and the geometrically computed \mathbf{n}_k vector, which is chosen parallel to the polarization vector. It was observed that, on average, these angles did not exceed 4° . This value is within the range considered acceptable for the noise in

polarization data, as described in the section on polarization data noise level.

- The WA parameter estimates depend strongly on the choice of α , the P-wave velocity in the reference medium, and especially the value of parameter ε_z , which is well estimated by this inversion scheme.

APPENDIX – SENSITIVITY MATRIX

The matrix presented in Eq. (7) consists of the left-hand side of that equation minus the WA parameters. It has as many rows as there are observations and as many columns as there are parameters. For the i -th observation, the i -th line of this matrix is given by,

$$\begin{aligned}
 M_{i1} &= \alpha n_{i1}^4 [2\alpha(\alpha^2 - \beta^2)n_{i3} - 1], & M_{i9} &= 2\alpha n_{i1}n_{i2}n_{i3}[\alpha(\alpha^2 - \beta^2)(2n_{i3}^2 - 1) - n_{i3}], \\
 M_{i2} &= \alpha n_{i2}^4 [2\alpha(\alpha^2 - \beta^2)n_{i3} - 1], & M_{i10} &= \alpha^3 n_{i1}[\alpha(\alpha^2 - \beta^2)(4n_{i3} - 1) - 2n_{i3}], \\
 M_{i3} &= -\alpha n_{i3}^3 [2\alpha(\alpha^2 - \beta^2)D^2 n_{i3}], & M_{i11} &= 2\alpha n_{i1}^3 n_{i2} [2\alpha(\alpha^2 - \beta^2)n_{i3} - 1], \\
 M_{i4} &= -\alpha n_{i1}^2 n_{i3} [2\alpha(\alpha^2 - \beta^2)D^2 n_{i3}], & M_{i12} &= \alpha n_{i2}^3 [\alpha(\alpha^2 - \beta^2)(4n_{i3} - 1) - 2n_{i3}], \\
 M_{i5} &= \alpha n_{i1}^2 n_{i3} [\alpha(\alpha^2 - \beta^2)(2n_{i3}^2 - 1) - n_{i3}], & M_{i13} &= 2\alpha n_{i2}^3 n_{i1} [2\alpha(\alpha^2 - \beta^2)n_{i3} - 1], \\
 M_{i6} &= \alpha n_{i1}^2 n_{i2}^2 [2\alpha(\alpha^2 - \beta^2)n_{i3} - 1], & M_{i14} &= \alpha n_{i3}^3 n_{i2} [\alpha(\alpha^2 - \beta^2)(4n_{i3} - 1) - 2], \\
 M_{i7} &= \alpha n_{i1}^2 n_{i2}^2 [\alpha(\alpha^2 - \beta^2)(4n_{i3}^2 - 1) - 2n_{i3}], & M_{i15} &= \alpha n_{i3}^3 n_{i1} [\alpha(\alpha^2 - \beta^2)(4n_{i3} - 3) - 2]. \\
 M_{i8} &= \alpha n_{i1}^2 n_{i1}^2 [\alpha(\alpha^2 - \beta^2)(4n_{i3} - 1) - 2n_{i3}], & &
 \end{aligned} \tag{17}$$

The elements are the i th components of the reference medium's polarization vector. Columns are sorted according to the order of the WA parameters in Eq. (8).

ACKNOWLEDGEMENTS

The authors thank the Post-Graduate Program on Geophysics of the Universidade Federal do Pará, CNPq and CAPES for the scientific initiation and Masters scholarships; Professor Ivan Pšenčík for the idea behind this work and Professors João Batista Correia da Silva and Jessé Costa for useful discussions.

REFERENCES

- AKI K & RICHARDS PG. 1980. Quantitative seismology, Theory and Methods. W.H. Freeman and Company, 700 pp.
- BARRETO AC, GOMES ENS, MACAMBIRA R & COSTA JC. 2013. Improvement of local anisotropy estimation from VSP data through experimental design. *Journal of Geophysics and Engineering*, 10: 1–12.
- FARRA V & PŠENČÍK I. 2003. Properties of the zeroth-, first- and higher-order approximations of attributes of elastic waves in weakly anisotropic media. *J. Acoust. Soc. Am.*, 114: 1366–1378.
- GAJEWSKI D & PŠENČÍK I. 1990. Vertical seismic profile synthetics by dynamic ray tracing in laterally varying layered anisotropic structures. *J. Geophys. Res.*, 67(1): 300–306.
- GOMES E, ZHENG X, PŠENČÍK I, HORNE S & LEANEY S. 2004. Local determination of weak anisotropy parameters from walkaway VSP qP-wave data in the Java Sea region. *Stud. Geophys. Geod.*, 48: 215–231.
- HELBIG K. 1994. Foundations of Anisotropy for Exploration Seismic. Oxford. Pergamon. Handbook of Geophysical Exploration, 22: 1698.
- HORNE SA & LEANEY WS. 2000. Polarization and slowness component inversion for TI anisotropy. *Geophysical Prospecting*, 48: 779–788.
- PŠENČÍK I & GAJEWSKI D. 1998. Polarization, phase velocity and NMO velocity of qP waves in arbitrary weakly anisotropic media. *Geophysics*, 63: 1754–1766.
- RUSMANUGROHO H & McMECHAN G. 2012. Sensitivity of estimated elastic moduli to completeness of wave type, measurement type, and illumination apertures at a receiver in multicomponent VSP data. *Geophysics*, 77: 1–18.
- SCHOENBERG M & DOUMA J. 1988. Elastic wave propagation in media with parallel fractures and aligned cracks. *Geophys. Eur. Assn. Geosci. Eng.*, 36: 571–590.
- THOMSEN L. 1986. Weak elastic anisotropy. *Geophysics*, 51(10): 1954–1966.
- ZHENG X & PŠENČÍK I. 2002. Local determination of weak anisotropy parameters from qP-wave slowness and particle motion measurements. *PAGEOPH*, 59, p. 1881–1905.

Recebido em 23 outubro, 2013 / Aceito em 8 setembro, 2014
Received on October 23, 2013 / Accepted on September 8, 2014

NOTES ABOUT THE AUTHORS

Raiza de Nazaré Assunção Macambira is graduated in Geophysics by Universidade Federal do Pará (2011), master degree in Geophysics by Universidade Federal do Pará (2013) specialized in seismic methods. Nowadays working for Schlumberger company as Field Geophysicist and in Ocean Bottom Cable surveys and processing seismic data in Rio de Janeiro office.

Ellen de Nazaré Souza Gomes has a degree in Mathematics from the Universidade da Amazônia (1990), M.Sc. in Mathematics (1999) and D.Sc. in Geophysics (2003), both from the Universidade Federal do Pará – UFPA. Currently, is Associate Professor at the Faculty of Geophysics and Coordinator of the Graduate Program in Geophysics at UFPA. Has experience in Geophysics, with emphasis on seismic methods, working on the following topics: seismic processing and anisotropy estimation.

Adriano César Rodrigues Barreto has a B.Sc. (2010) and a M.Sc. (2012) degrees in Geophysics from the Universidade Federal do Pará, with specialization on seismic methods. Also has experience in other geophysical methods, like gravity and magnetics, and electrical and electromagnetic methods. Currently, is a Junior Geophysicists at Petrobras.